


## AUTHOR QUERY FORM

 <b>ELSEVIER</b>	<b>Journal: SUSC</b>  <b>Article Number: 19988</b>	<b>Please e-mail or fax your responses and any corrections to:</b> <b>Balan, Rohit</b> <b>E-mail: <a href="mailto:Corrections.ESCH@elsevier.spitech.com">Corrections.ESCH@elsevier.spitech.com</a></b> <b>Fax: +1 619 699 6721</b>
--	--	---

Dear Author,

Please check your proof carefully and mark all corrections at the appropriate place in the proof (e.g., by using on-screen annotation in the PDF file) or compile them in a separate list. Note: if you opt to annotate the file with software other than Adobe Reader then please also highlight the appropriate place in the PDF file. To ensure fast publication of your paper please return your corrections within 48 hours.

For correction or revision of any artwork, please consult <http://www.elsevier.com/artworkinstructions>.

Any queries or remarks that have arisen during the processing of your manuscript are listed below and highlighted by flags in the proof. Click on the 'Q' link to go to the location in the proof.

<b>Location in article</b>	<b>Query / Remark: <a href="#">click on the Q link to go</a> Please insert your reply or correction at the corresponding line in the proof</b>
<a href="#">Q1</a>	Please confirm that given names and surnames have been identified correctly.
<a href="#">Q2</a>	Please check the telephone and fax number of the corresponding author, and correct if necessary.
<a href="#">Q3</a>	Please check the edit(s) made in the sentence "In these parameter choices we are guided by previous studies on Al/Si(100), both theoretical [40] and experimental [46]...", and correct if necessary.
<a href="#">Q4</a>	Please check the edit(s) made in the sentence "having been formed at low coverages they simply have more time to aggregate and thus shifting the island size distribution slightly toward larger sizes...", and correct if necessary.
<a href="#">Q5</a>	Uncited reference: This section comprises references that occur in the reference list but not in the body of the text. Please position each reference in the text or, alternatively, delete it. Thank you. <div data-bbox="639 1377 1148 1495" style="border: 1px solid black; padding: 10px; margin: 10px auto; width: fit-content;">             Please check this box if you have no corrections to make to the PDF file. <input type="checkbox"/> </div>

Thank you for your assistance.



ELSEVIER

Contents lists available at SciVerse ScienceDirect

## Surface Science

journal homepage: [www.elsevier.com/locate/susc](http://www.elsevier.com/locate/susc)

## Highlights

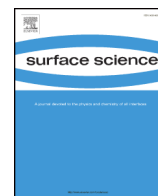
**Enhanced nucleation of Al islands on H-dosed Si(100)-2 × 1 surface:  
A combined density functional theory and kinetic Monte Carlo study***Surface Science xxx (2013) xxx–xxx*Marvin A. Albao<sup>a,\*</sup>, Darwin B. Putungan<sup>a</sup>, Chia-Hsiu Hsu<sup>b</sup>, Feng-Chuan Chuang<sup>b,\*</sup><sup>a</sup> *Institute of Mathematical Sciences and Physics, University of the Philippines Los Baños, 4031, Philippines*<sup>b</sup> *Department of Physics, National Sun Yat-Sen University, Kaohsiung 804, Taiwan*

- Blocking of Al adatoms by H impurities on H-dosed Si(100) enhances Al island density.
- Heterogeneous Al islands outnumber homogeneous islands but not totally dominant.
- Aggregation on either side of H possible but very unlikely for low Al coverages.
- Al monomer density elevated, leading to persistent nucleation
- Binding energy between H and Al most likely no more than 0.2 eV



Contents lists available at SciVerse ScienceDirect

Surface Science

journal homepage: [www.elsevier.com/locate/susc](http://www.elsevier.com/locate/susc)

# Enhanced nucleation of Al islands on H-dosed Si(100)-2 × 1 surface: A combined density functional theory and kinetic Monte Carlo study

Marvin A. Albao<sup>a,\*</sup>, Darwin B. Putungan<sup>a</sup>, Chia-Hsiu Hsu<sup>b</sup>, Feng-Chuan Chuang<sup>b,\*</sup>

<sup>a</sup> Institute of Mathematical Sciences and Physics, University of the Philippines Los Baños, 4031, Philippines

<sup>b</sup> Department of Physics, National Sun Yat-Sen University, Kaohsiung 804, Taiwan

## ARTICLE INFO

### Article history:

Received 23 March 2013

Accepted 3 July 2013

Available online xxxx

### Keywords:

First-principles calculations

Kinetic Monte Carlo simulations

Aluminum

Si(100)

One-dimensional islands

## ABSTRACT

Using a combined density functional theory (DFT) and kinetic Monte Carlo (kMC) approach, we show that the presence of small dose of hydrogen atoms on Si(100)-2 × 1 surface can increase Al chain density by as much as four times compared to the clean Si(100)-2 × 1 value. Though the observed enhanced nucleation can be explained by trapping of Al adatoms by H and their subsequent stabilization into islands, we find that a similar increase in island density can be achieved even when H merely blocks (but does not trap) Al adatoms. For H-bound islands, our DFT analysis suggests that Al adatoms are pinned preferentially on one side of H. Additionally, we argue that despite the high ratio of diffusion to adsorption rates which should favor H-bound islands over homogeneously nucleated islands, the former is not as numerous conventional nucleation theory would predict.

© 2013 Published by Elsevier B.V.

## 1. Introduction

Advances in nanolithography which make it possible to tailor a substrate of interest to produce surfaces with the right transport, mechanical, and electrical properties: nanostructuring at a truly atomic scale, have progressively increased to the point of commercial viability [1,2]. To this end, an array of techniques, ranging from the relatively simple, such as self-assembly, to one requiring active manipulation at the atomic scale, has been successfully applied. In self-assembly, the physical properties of thin films grown on the substrate such as the aggregates' island size and island density are controlled by physical parameters such as substrate temperature and adsorption rate [3,4]. However, precise placement on the substrate to fit a desired pattern, a necessary requirement in nanocircuit design, may not always be achievable using this technique. This is true in the case of an important class of one-dimensional (1D) islands, or nanowires, formed during room-temperature (RT) deposition of group III and IV metals [5–8], several transition metals (Mn, Pb) [9–11], mixed In–Sn and Pb–Al dimers [12,13], and most rare-earth silicides [14–16] on Si(100). On the other hand, scanning probe lithography techniques allow surface atoms to be manipulated at the atomic level using scanning tunneling microscope (STM) tip by selectively placing or removing atoms (or even a row of atoms) from their adsorption sites at will. For example, nanopatterning [17–19] is achieved by removing and manipulating hydrogen atoms on low-index semiconductor surfaces and thus leaving dangling bonds as attractive nucleation sites. Electronic structure

analysis can then be performed. A similar approach on vicinal surfaces, step decoration [20,21], takes advantage of the increased ability to produce terraces of very precise width, sometimes of the order of a few atoms. Coupled with highly reactive surface steps, one could produce 1D or quasi-1D nanostructures which are constrained to align along the step direction. In this work, we explore a potential approach toward a more controlled self-assembly process through deliberate introduction of impurities in the form of pre-adsorbed H atoms, a common surface residue on Si-based surfaces.

In Ref. [22] it was observed that dosing the Si(100)-2 × 1 surface with a small amount of hydrogen (~0.15 ML) before deposition of Al significantly alters the nucleation rate of Al islands. One of the mechanisms the authors considered is the trapping of the highly-mobile adatoms by the largely stationary atomic H and the subsequent stabilization of these atoms into heterogeneous 1D islands. (Henceforth, heterogeneously nucleated islands, or simply heterogeneous islands, will be used interchangeably with H-bound islands.) This behavior is reminiscent of the role C-defects, believed to be dissociated water molecule adsorbed on adjacent Si dimers [23], during adsorption and nucleation of other group III metals on Si(100)-2 × 1, notably In [24]. A second, perhaps complementary mechanism they proposed somewhat diminishes the role of H in that it is unable to trap these fast diffusing Al adatoms, but can nevertheless block their path. In this scenario, H atom's site-blocking role likely raises the number of diffusing Al adatom available for pairing with other mobile adatoms to produce a stable Al dimer, the building block for homogeneously nucleated 1D island. This possibility is easily verified by looking at the experimental data and examining the size distribution of the islands which should show an abundance of homogeneous 1D islands in addition to H-bound 1D islands.

\* Corresponding authors. Tel.: +886 7 5625 3733; fax: +886 7 5253709.

E-mail addresses: [maalbao@uplb.edu.ph](mailto:maalbao@uplb.edu.ph) (M.A. Albao), [fchuang@mail.nsysu.edu.tw](mailto:fchuang@mail.nsysu.edu.tw) (F.-C. Chuang).

The present work, employing first-principles based kinetic Monte Carlo simulations, is intended to shed more light on the role of H on the observed enhanced nucleation of Al islands by comparing model predictions with available experimental data on the size distribution as well as the island density. It should be remarked that any attempt at direct observation of H-mediated nucleation via STM or other imaging techniques faces formidable technical challenges. Thus, kMC modeling of a suitable growth model for Al chains on Si(100)- $2 \times 1$  is needed for additional insights into the process. This paper is organized as follows. In Sec. 2, we investigate whether the presence of H atoms can indeed trap adjacent Al adatoms by calculating the relevant adsorption energies using DFT. An important question, whether islands nucleate on either side of an H atom, will be discussed. In Sec. 3, we incorporate results of our DFT calculations, as well as relevant key observations from relevant experimental studies, into the current modeling, and discuss how the mere presence of H atoms plausibly enhances Al island nucleation. In Sec. 4, we summarize the main points of the article.

## 2. DFT calculations: Methodology and results

### 2.1. Methodology

To accurately model the evolution of any surface of interest during molecular beam epitaxy (MBE) or physical vapor deposition (PVD) one needs a good understanding of the microscopic processes involved as well as an accurate determination of the relevant energetic and kinetic parameters. Such a detailed knowledge of the surface processes typically comes from experimental observations and first-principles calculations. In this section, we provide a description of our DFT-based methodology, where our main goal is to establish whether hydrogen can act as pinning center for diffusing Al adatoms.

In our previous work on the self-assembly of group III metals on Si(100)- $2 \times 1$  [25], progress has been made in generating a potential energy surface (PES) map from which one can (1) identify transition and metastable states as well as saddle points (2) calculate the associated activation barriers for a chosen pathway (3) analyze the stability of various island structures in the immediate vicinity of defects by looking at their relevant adsorption energies. We wish to replicate such calculations to Si(100)- $2 \times 1$  surface with H taking the place of defects.

Our calculations were carried out within the generalized gradient approximation (PBE) [26] to density functional theory [27] using projector-augmented-wave potentials [28], as implemented in Vienna Ab-Initio Simulation Package [29]. Since the 1D island is elongated along the [011] direction, we used the  $8 \times 4$  supercell as the slab substrate and manipulated the  $c(4 \times 2)$  at the reconstruction layer. The use of a larger supercell ( $8 \times 4$ ) is intended to prevent interaction between metal atoms of adjacent cells. The  $1 \times 2$  Monkhorst-Pack grid was employed to sample the surface Brillouin-zone (BZ). The calculation settings are described in previous works [25,32] and will not be elaborated here.

### 2.2. DFT results

Among the notable prior works on H adsorption on Si(100) is a study examining Si dangling bond creation via H adsorption on dimerized Si(100) which established that forming Si-Si-H hemihydride can induce static buckling on adjacent Si-Si dimers [30]. Additionally, it was found that the created single dangling bond's electronic structure depends on the doping properties of the surface, giving different Si-H bonding geometries with distinct scattering and transport properties [31].

In the present study, our aim is primarily to understand nucleation and growth of 1D Al islands on H/Si(100). Previously, it was reported that group III metals (notably In) can be trapped in varying degrees by C-defects [32,24,33]. Whether a similar process occurs when an Al adatom lands next to atomic H is not clear, although surface defects

in the form of missing dimers or C-defects have been observed to terminate Al islands [34,35]. As a preliminary step, we need to find possible adsorption sites: local minima on the PES, on the Si(100)- $2 \times 1$  surface for H.

#### 2.2.1. H adsorption on clean Si(100)

In Fig. 1a–c, the two Si atoms constituting a dimer, which we labeled as *up* or *down*, are represented by red and blue balls, respectively. Such a distinction between otherwise identical atoms is necessitated by fact that the Si dimer is slightly tilted with respect to the horizontal rather than flat. Since H can be adsorbed on top of either type of Si atom it is instructive to compare their respective energies.

We find that H favors adsorption on the *up* Si atom rather than the *down* by 0.052 eV on a clean Si(100) surface. Since we used the  $c(4 \times 2)$  reconstruction, the position (relative to a Si dimer) of the marginally more stable adsorption site for H (*up* Si atom) along the dimer row alternates from right to left, i.e., it follows a zigzag pattern.

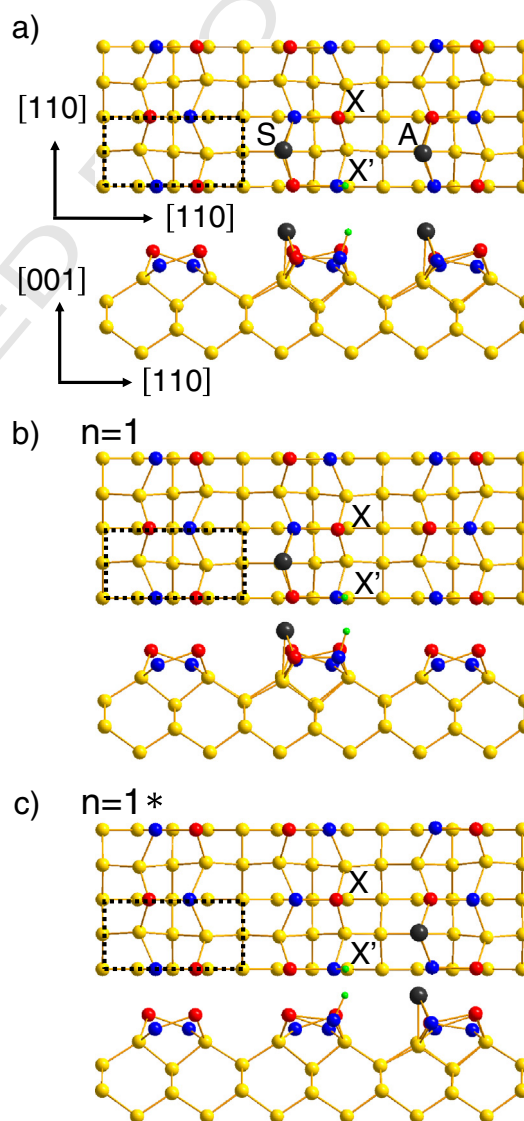


**Fig. 1.** (a) X and X' indicate adsorption sites for H located on top of an *up* Si atom (red ball) and a *down* Si atom (blue ball), respectively. S and A denote adsorption sites for the first Al atom (black ball) adsorbed next to H (green ball). Notice that S is on the same dimer row, while A is on the adjacent dimer row, as X and X'. (b) Shows top and side views of an Al atom adsorbed on S, while (c) shows top and side views of an Al atom adsorbed on A. In these figures, yellow balls indicate substrate Si atoms while black dash lines outline the  $2 \times 1$  supercell. (For interpretation of the references to color in this figure legend, the reader is referred to the web version of this article.)

In Fig. 1a, X indicates binding site for H in which it is bonded to an up Si atom while X' marks a slightly less stable adsorption site for H where it is bonded to a down Si atom.

### 2.2.2. Al adsorption on H-dosed Si(100)-2 × 1

To compare the relative stabilities of various heterogeneously nucleated 1D Al islands, we calculate the adsorption energy of the last Al atom to be incorporated in the island, defined as follows:

$$\Delta E_{n,ads}^0 = E_n^0 - E_{n-1}^0 - \mu_{Al} \quad (1)$$

$$\Delta E_{n,ads}^{H/CD} = E_n^{H/CD} - E_{n-1}^{H/CD} - \mu_{Al} \quad (2)$$

In Eq. (1),  $\Delta E_{n,ads}^0$  denotes the adsorption energy of the  $n$ th Al adatom in an island of length  $n$  on the clean Si(100)-c(4 × 2) while  $E_n^0$  is the total energy of an island of length  $n$  plus the underlying Si substrate. Similarly, in Eq. (2),  $\Delta E_{n,ads}^{H/CD}$  denotes the adsorption energy of the  $n$ th Al adatom in a H/C-defect-bound island of length  $n$  on the Si(100)-c(4 × 2) surface, while  $E_n^{H/CD}$  gives the corresponding total energy of an  $n$ -atom island attached to H/C-defect (plus substrate). In the above equations,  $\mu_{Al}$ , the chemical potential of Al, is chosen to be that of an isolated Al atom in vacuum. According to these definitions, lower (or more negative) values of the adsorption energy for Al adatoms implies greater stability.

In Table 1 we present calculated values of the adsorption energies of Al atoms terminating H-bound islands of various sizes, ranging from 1 to 4. From the table, it is apparent that the adsorption energy of Al depends on whether H is bonded to an up or down Si atom, i.e., H is at X or X'. To simplify our subsequent discussions below, we assume (unless noted otherwise) that H is bonded to a down Si atom.

Previous studies [32,36] have identified the M site, an off-center site in which an Al atom is bound to two Si atoms, as the most stable among the different candidate binding sites for adsorption of Al on bare surface Si(100), which includes pedestal, bridge and cave sites. In the presence of H, we expect the existence of candidate binding sites that are very close to the aforementioned original binding sites. Indeed, our calculations have identified stable sites near the M-site that are either on the same dimer row where H is adsorbed (in the case of the site S) or in the adjacent dimer row (in the case of labeled A) as shown in Fig. 1a. Between the two, adsorption on S sites (Fig. 1b) is more stable than on A (Fig. 1c), with the former having an adsorption energy of -3.517 eV versus the latter's -3.051 eV. (Note however, that in the absence of H these sites become equivalent).

As we shall see later, the observation that adsorption on S is more stable than that in A has important implications on the preferential direction for nucleation and growth of H-bound islands. Additionally, from Table 1, one concludes that, compared with a C-defect, H is a slightly better trap for an Al adatom since the adsorption energy of an H-bound Al adatom is slightly lower than that adsorbed next to a C-defect.

For  $n = 2$ , it is evident from Table 1 that a dimer termination (Fig. 2a) is generally more stable than atom termination (Fig. 1b). For example, Table 1 reveals that when H is bonded to the down Si atom,

the adsorption energy of the former is -3.994 eV while that in Fig. 1b is -3.517 eV, a difference of around 0.48 eV. This is consistent with the finding in Ref. [34] which revealed that most of the islands appear to be dimer terminated based on detailed analysis of STM images. Next, we analyzed another structure for  $n = 2$  (shown in Fig 2b) where the second Al adatom is positioned across the trench on the opposite side of H as the first Al adatom and has an adsorption energy of -2.947 eV. We found that this structure is less stable than that shown in Fig. 2a by about 1.05 eV.

One could argue that because this difference is large, further growth proceeds on the side of H where the first adatom is already pinned. Effectively, this means growth on the other side of H is suppressed, at least at low coverages. Furthermore, we observe that the adsorption energy of the second adatom on this side is roughly the same as that of the free Al adatom (-2.923 eV). This suggests that if the second atom were to bind to H at all, the binding energy,  $E'_{Al-H}$ , will have to be negligibly small. However, if a third adatom arrives to form a dimer with the second adatom before the latter has a chance to diffuse elsewhere, the resulting 1D island could grow on both sides of H.

To examine the likelihood of this scenario, we compare the time elapsed between successive arrivals of two adatoms on the same H atom, roughly  $\Delta t = n_H/F$  with the resident time the second adatom on H,  $t_H = v^{-1} e^{(E_{Al-H} + E_d)/kT}$  [37]. In the above,  $n_H$  is the impurity concentration,  $F$  is the adsorption rate,  $v$  is the hopping pre-factor, while  $E_d$  is the diffusion barrier of isolated Al adatom. Since the Si(100)-2 × 1 surface is anisotropic, we simply approximated  $E_d$  by  $E_{||} = 0.31$  eV, the activation barrier for migration along the "fast" direction, i.e., along the Si dimer row. Thus, with  $n_H = 0.15$  (per site),  $F = 0.001$  ML/s,  $E'_{Al-H} = 0$ ,  $\Delta t \sim 150$  s while  $t_H \sim 10^{-9}$  s. Obviously, since  $\Delta t \gg t_H$ , the above-mentioned scenario could be discounted, and growth is likely limited on the side where the first Al adatom is already bound to H. This feature is reminiscent of the growth of group III metals near C-defects on Si(100)-2 × 1 surface, a finding initially reported in Ref. [24].

Next, for  $n = 3$  we placed a third Al adatom on a stable adsorption site (M site) near a H-bound dimer. After the relaxation using conjugated gradient method, we found that such an adatom subsequently drifts away from M site and shifts toward the right and binds to the metal dimer as shown in Fig. 2c. Our calculations indicate that this structure where the third Al adatom is bonded to the dimer close to H@down (H@up) is more stable than one in which the same adatom is placed at the M site as shown in Fig. 2d [38] by about 0.22 eV (0.32 eV). We note that in order to obtain Fig. 2d we allow the third adatom to relax along the y and z directions while fixing its x-position, where x and y refer to directions orthogonal and parallel to the Si dimer row, respectively, while z refers to the vertical direction. Here, H@down(H@up) refers to H that is bonded to a down (up) Si atom and has an adsorption energy given by -3.369 eV (-3.232 eV).

The lowest energy structure for  $n = 4$  is shown in Fig. 2e, where four Al atoms form two Al dimers. Another possible configuration (labeled  $n = 4^*$ ) can be generated by using the optimized structure for  $n = 3$  (Fig. 2c) as a starting point, adding a fourth Al adatom and then allowing the system to relax. The resulting structure is shown in Fig. 2f, and has a higher energy compared to Fig. 2e (by 1.27 eV). This

**Table 1**

The adsorption energies (in eV) of Al adatoms chain terminating different 1D island structures, C-defect-bound, H-bound, and free (e.g. unbound). C-defect-bound values shown here are adopted from our previous calculations reported in Ref. [25]. (\*) denotes alternative, stable structures that are typically higher in energy than the optimized structures.

Model	$n = 1$	$n = 1^*$	$n = 2$	$n = 2^*$	$n = 3$	$n = 3$	$n = 4$	$n = 4^*$
	No bonding							
Fig.	(1b)	(1c)	(2a)	(2b)	(2c)	(2d)	(2e)	(2f)
Free	-2.923		-4.303		-3.476		-4.283	
C-defect	-3.298	-2.933	-4.523		-3.471	-3.232	-4.291	
H@down bound	-3.517	-3.051	-3.994	-2.947	-3.589	-3.369	-4.165	-2.592
H@up bound	-3.371	-2.558	-4.090	-2.939	-3.547	-3.232	-4.209	-2.920

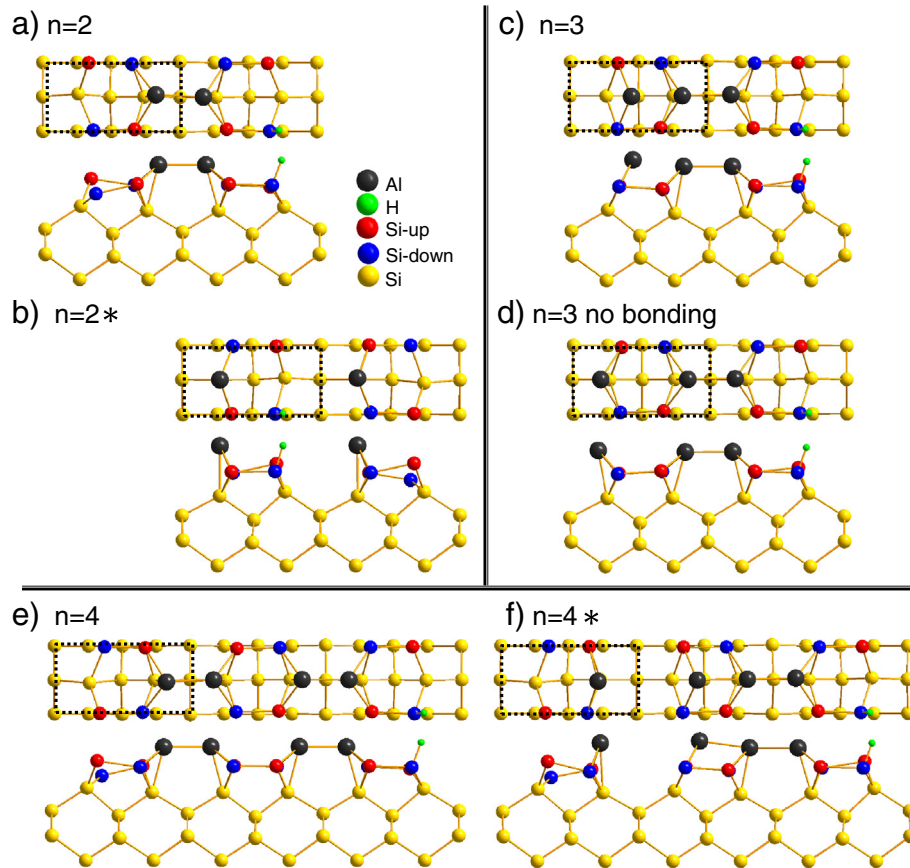


**Fig. 2.** (a) Optimized atomic structure for an H-bound Al dimer in the case  $n = 2$ . (b) An alternative structure for  $n = 2$  where the two Al atoms are placed on either side of H at sites S and A and has a total energy that is 1.05 eV higher than the structure in (a). (c) Optimized atomic structure for  $n = 3$ . (d) An alternative structure for  $n = 3$  in which the third Al adatom is placed at the M-site. (e) Optimized atomic structure for  $n = 4$ , and (f) An alternative structure ( $n = 4^*$ ) that is higher in energy than that shown in (d) by around 1.27 eV. In all these cases, top and side view of the structures are shown.

means that an energy barrier needs to be overcome if Fig. 2f is to transform into Fig. 2e. In order to obtain this energy barrier, the x position of the third Al adatom is gridded along the path joining Fig. 2f to e by 0.1 Å. The relaxations were done for each grid point provided that the x positions of both the third and fourth Al adatom are fixed. We found that this energy barrier is 0.13 eV from analysis of the PES map.

Note that the adsorption energy of the fourth Al adatom in Fig. 2e is only slightly greater than that of an atom in a free Al dimer, indicating that the influence of H extends up to the fourth atom (of the second dimer). Since the difference in the adsorption energy is around 3% or less, we conclude that the adsorption energies of the fourth Al adatom listed in Table 1 (4.209 eV and 4.165 eV for H@down-bound and H@up-bound islands, respectively) must be very close to the adsorption energy of last adatom in even-sized islands with  $n > 4$ . Owing to this closeness in values of the adsorption energy, and the fact that any additional calculations for island sizes  $n > 4$  are much more computationally expensive, extending our analysis beyond  $n = 4$  is neither practical nor necessary. We should also point out that a similar study involving C-defect bound islands indicates that the impact of C-defects on the adsorption energy of the fourth atom in the second dimer is not significant [33].

### 3. Atomistic lattice-gas model description and kMC simulation results

#### 3.1. Growth model details

The Si(100)- $2 \times 1$  surface consists of rows of dimers oriented along the [011] direction, with adjacent dimers within a row separated by

3.84 Å. Despite its inherent anisotropy, one can effectively model this surface by a square lattice of  $n \times n$  sites onto which the adsorbate of choice are deposited and adsorbed [39]. It should be stressed that since the surface is only sparsely populated with H atoms – the anisotropy of the underlying Si(100)- $2 \times 1$  structure is intact. Consequently, diffusion on this surface is likely anisotropic, though there is no general agreement [40–43,35] as to which principal direction (in relation to the Si dimer row) is diffusion considered faster. In contrast, a related study of Al diffusion on H-terminated Si(100) surface [43] in which H atoms saturates the dangling bonds of the underlying Si(100)- $2 \times 1$  surface thereby destroying the diffusional anisotropy in the process, leads to 2D Al islands rather than 1D atomic wires.

In addition, rate  $r$  of thermally activated processes on the surface such as diffusion are assumed to be governed by Arrhenius law,  $r = v e^{-E/kT}$ , where  $v$  is hopping pre-factor, typically chosen to be within  $10^{12}$ – $10^{13} \text{ s}^{-1}$  range,  $E$  is the activation barrier for the process, and  $T$  is the temperature.

In the current model, hydrogen atoms do not hop nor do they desorb, owing to the relative high barriers [44] for diffusion (as much as 2.72 eV and 1.65 eV for diffusion perpendicular and parallel to the Si dimer row, respectively) and an even higher barrier for desorption compared to the corresponding barriers associated with Al. At the start of the simulation, a low dose (0.15 ML) of H atoms are randomly deposited onto the lattice of  $n \times n$  sites. According to our discussion above, once adsorbed these atoms are considered immobile and therefore permanently occupy that site. What follows are the deposition, diffusion and nucleation of Al adatoms into homogeneous or H-bound islands and the competing processes of aggregation and adatom detachment. A glimpse of the typical surface morphology is

best illustrated in the schematic diagram shown in Fig. 3a, which also captures all the essential elements of the atomistic lattice-gas model employed in this work. The parallel-dimer structure [40,41,5], universally seen as the structure governing the growth of group III metals on Si(100)- $2 \times 1$ , is also included in Fig. 3b. A complete description of our model is provided below:

- (a) *Deposition of Al atom.* A site is randomly picked and an atom is deposited on it provided such a site is empty and not “forbidden” (i.e., sites laterally adjacent to an island or adatom). The existence of forbidden sites was first noted in a prior work [42], where we concluded from analyses of detailed STM images that these so-called forbidden sites are not favorable for adatom adsorption. Exceptions, however, have been noted in [45].
- (b) *Diffusion, nucleation, and aggregation.* In our modeling, Al adatoms undergo anisotropic diffusion, parallel, or orthogonal to the Si dimer row, until they reaches impurity (H) sites, meet other adatoms, or get incorporated into existing islands. The barrier for isolated adatom diffusion, along, and perpendicular to the Si dimer row is given by  $E_{\parallel} = 0.31$  eV and  $E^{\perp} = 0.47$  eV, respectively [25]. Also, there is an effective binding energy between H and an adatom,  $E^t$ , an adjustable parameter in our model. This key quantity determines whether H can pin diffusing Al adatoms long enough for a second atom to come in and thus stabilize the

resulting structure into an H-bound island, or to simply block their path without stabilization. Thus, this important parameter controls the extent in which heterogeneous (H-mediated) nucleation can occur. In addition to (reversible) heterogeneous nucleation, islands may also nucleate (reversibly) whenever two diffusing adatoms in the same metal row become adjacent to form a dimer nuclei (homogeneous nucleation).

In the model, successful (heterogeneous) nucleation occurs whenever a diffusing Al adatom finds itself next to an H atom in the same metal row. Notice that it is possible to approach an H atom that is already bound to an Al adatom from the “free” side, but that no aggregation follows since according to our discussion in Sec. II the adsorption energy of the second atom is high. In this case, H atom has no other function other than to block diffusing Al atoms. Later, we will explore the consequence of site-blocking to the evolution of the Al island density, as well as the balance between heterogeneous and homogeneous islands.

- (c) *Reversible detachment of Al adatoms.* As mentioned above, there is a binding energy between a hydrogen and Al adatom,  $E_t$ , treated as an adjustable parameter, ranging from 0 to 0.3 eV. The relatively low values are consistent with reversible capture of adatoms at H sites. In addition, Al adatoms detach reversibly from island ends (both H-bound and free) at rates given by  $h = \nu e^{-(E_{bind}+E_d)/kT}$  in which the binding energies,  $E_{bind}$ , are 1.1 eV (0.2 eV) for even-sized (odd-sized) islands. In these parameter choices we are guided by previous studies on Al/Si(100), both theoretical [40] and experimental [46]. We should stress, however, that these values are not intended to be exact, as the absolute accuracy of the aforementioned sources are not known. We also acknowledge that model simplifications contribute to the overall uncertainty in the binding energies. For example, the value  $E_{bind} = 1.1$  eV reported in Ref. [40], the energy needed to break up a homogeneously nucleated dimer, was the same value used in our simulations for all types of even sized islands (homogeneous and heterogeneous). Despite these obvious simplifications [47], we contend that using the dimer formation energy as the binding energy for even-sized islands is a good approximation for islands whose sizes are larger than 4, since it is expected that the influence of H on the binding energy weakens with increasing island size. Furthermore, consistent with our findings regarding the relative instability of odd-size islands as compared with the more stable even-size islands (both homogeneous or heterogeneous), as well as the experimental observation in Ref. [46] in which they concluded that most Al islands on Si(100) are dimer terminated, we used a binding energy 0.2 eV for the former. Again, this value is arbitrary to a large extent, but is sufficiently low to ensure that most islands are dimer terminated as observed in the simulations.

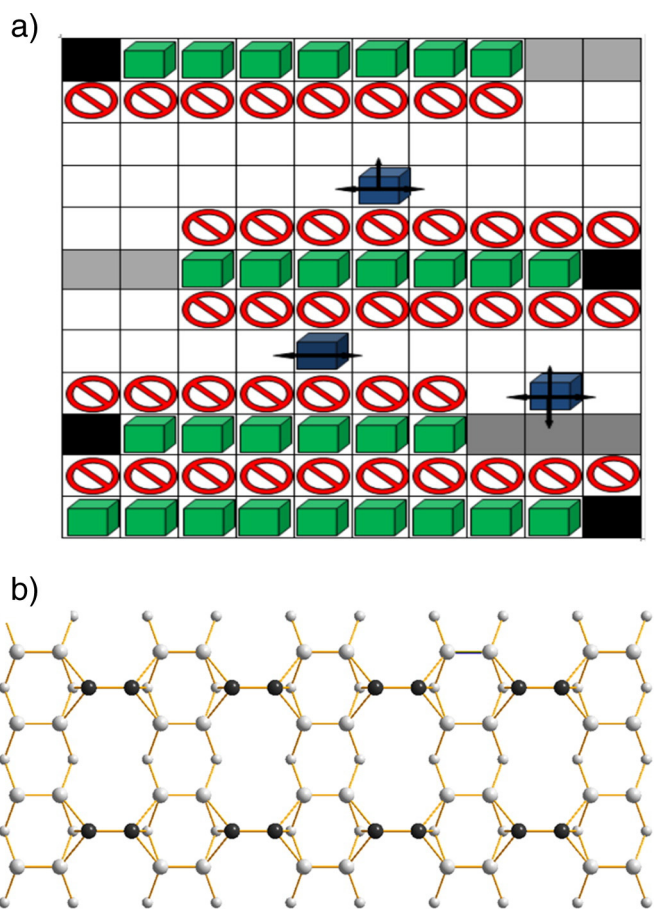


**Fig. 3.** (a) Illustration of the atomistic lattice-gas model. Each square in the grid represents potential binding sites for H and Al adatoms. Black squares indicate H sites next to which rapidly diffusing Al adatoms (blue cubes) can be trapped or blocked. Green cubes represent Al adatoms in atomic chains. Gray squares found at the end of these chains indicate aggregation sites for Al, while squares with red signage indicate forbidden sites for atomic chain formation. (b) The parallel dimer model, where adatom chains (black balls) are formed perpendicular to the Si dimer rows (white balls). (For interpretation of the references to color in this figure legend, the reader is referred to the web version of this article.)

### 3.2. kMC simulation results

To mimic experimental conditions in [22], we set the substrate temperature to 373 K and the adsorption rate to 0.5 ML/min while performing several independent runs using a  $300 \times 300$  lattice grid. (Our tests indicate that the choice of the lattice size ( $300 \times 300$ ) should be big enough to avoid any finite-size effects). Prior to Al deposition, the Si(100) surface was pre-dosed with 0.15 ML hydrogen at random sites. In the case of clean growth, we add very small concentration of C-defects, around 0.003 ML, instead of H. In the simulations, data gathering starts once Al coverage of 0.1 ML is reached. Various plots were then obtained and Al thin film morphologies generated for different values of  $E_t$ .

In Fig. 4a, we plotted the island density per site as a function of  $E_t$  and also broke it down by island type (homogeneous or heterogeneous). In general, these plots reveal that the overall island density gradually

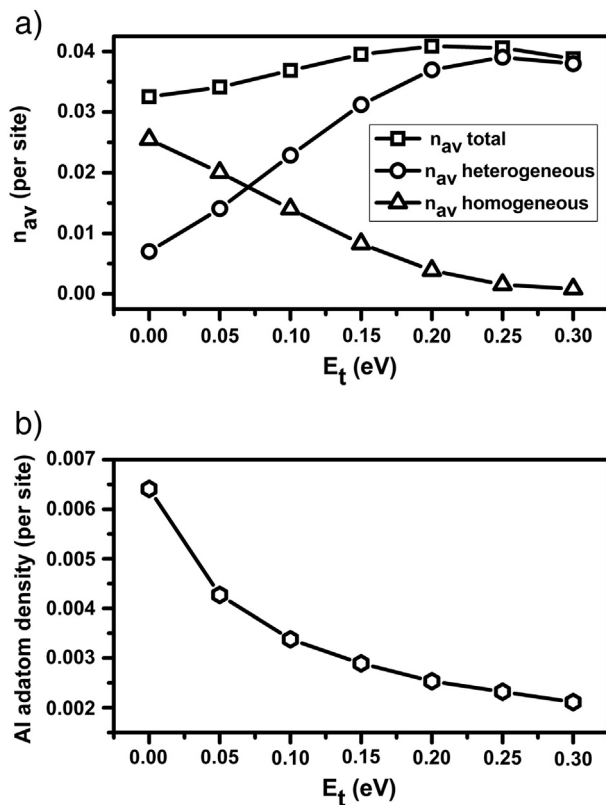


Fig. 4. (a) Uppermost plot shows dependence of total island density (per site),  $n_{av,total}$  on  $E_t$  (square). Additional insights provided by similar plots showing dependence of homogeneous island density (per site),  $n_{av,homogeneous}$  (triangle) and heterogeneous island density (per site),  $n_{av,heterogeneous}$  (circle) on  $E_t$ ; (b) shows variation of Al adatom density(per site) with  $E_t$ .

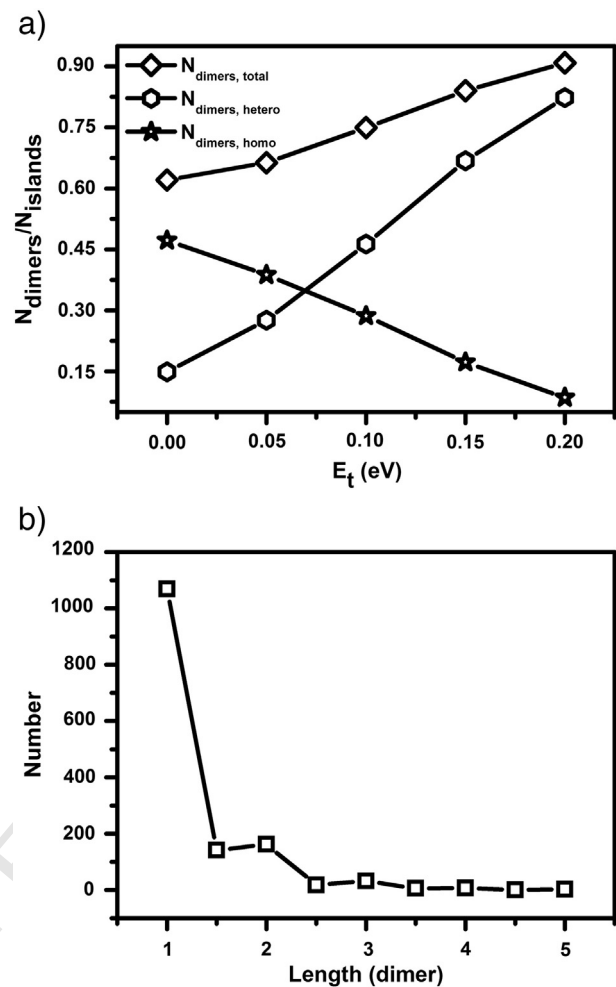


Fig. 5. (a) Uppermost plot shows fraction of dimers among the islands,  $N_{dimers,total}$  on the surface (diamond) as a function of  $E_t$ . Lower plots reveal fraction of heterogeneous,  $N_{dimers,hetero}$  (pentagon) and homogeneous dimers,  $N_{dimers,homo}$  (star) among the islands on the surface as a function of  $E_t$ . (b) Island size distribution for  $E_t = 0.1$  eV.

increases with  $E_t$ , suggesting that overall nucleation rate is indeed boosted with the increase in  $E_t$ . Here, analysis of simulation data reveals that the ratio of the island density to the clean growth value [48] for  $E^f > 0.0$  [0.05 eV–0.3 eV] has a maximum value of 4.35 when  $E^f = 0.2$  eV. This finding is in line with experimental data in Ref. [22] where they observed five times more Al islands on the H-dosed surface compared to those grown on clean Si(100)- $2 \times 1$  surface. In contrast, this same quantity is only 3.46 when  $E_t = 0$ , a figure that is nevertheless in fair agreement with experimental result.

It is also interesting to note the behavior of the density of islands formed via different nucleation pathway (heterogeneous or homogeneous) as can be deduced from the plots. While homogeneous islands are slightly favored for very small values of  $E_t$ , starting at 0.07 eV heterogeneous islands start to outnumber homogeneous islands. Indeed, when trapping efficiency of adatoms by H is low (such as the case at low  $E_t$ ), most of the excess adatoms simply form dimers thereby increasing the number of homogeneous islands (relative to heterogeneous islands). This much can be inferred from Fig. 4b, showing the plot of adatom density(per site) with  $E_t$ , and Fig. 5a, which independently allows us to quantify the impact of  $E_t$  on island statistics by showing the fraction of dimers among the islands, broken down by type (H-bound or free).

These preceding results highlight one important point: enhanced nucleation can be achieved by the mere presence of impurities, even if the adatoms are only weakly bound to the impurities. In the case of negligibly small binding between adatom and impurity, such an increase in island density may be achieved through formation of homogeneously nucleated islands.

In Fig. 5a, it is notable that the percentage of dimers among the 1D islands decreases with  $E_t$ , ranging from 88% for  $E_t = 0.2$  eV to 62% for  $E_t = 0.0$  eV. The trend is better understood in light of the observation

that when  $E_t$  approaches zero, the average size of the predominantly homogeneous islands becomes larger, while island density becomes smaller. Plausibly, homogeneous islands that nucleate when  $E_t$  is low are typically older – having been formed at low coverages they simply have more time to aggregate and thus shifting the island size distribution slightly toward larger sizes. Notice that for  $E_t = 0.1$  eV, the corresponding figure is 75%. This matches well with the experimental value given in Ref. [22] in which the authors reported that dimers account for up to 75% of all the islands in some areas of the terrace. (We take this to mean that 75% is the upper limit rather than an average value). To complete the picture we have provided in Fig. 5b a size distribution of 1D Al islands for 0.1 ML deposition and with  $E_t = 0.1$  eV. Notice that since even-sized islands typically outnumber the less stable odd-sized islands, the size distribution is neither monotonically decreasing nor monomodal in form, though it resembles the former more than the latter. Monotonically decreasing size distribution is a common feature found in related deposition systems such as Ga/Si(100) [42] and In/Si(100) [49].

Overall, our analysis points to 0.1 eV as perhaps the optimum choice for  $E_t$ , based on comparison between model predictions and the corresponding experimental data on the ratio of the island density on H-dosed to that on clean Si(100)- $2 \times 1$  surface, as well as the fraction of islands which are dimers. We emphasize that even though we believe this is the optimum choice, the true value of  $E_t$  may lie somewhere in the range [0.05 eV, 0.2 eV].

Surprisingly, although heterogeneous nucleation is more prevalent (relative to homogeneous nucleation) except for very small values of  $E_t = 0.05$  eV (or less), it is not completely dominant. In fact, they remain within the same order of magnitude for sufficiently low values of  $E_t$  considered here. This result is even more remarkable when we realize that the hydrogen concentration (0.15 ML) is much higher than that of the typical impurity. Ordinarily, mean-field nucleation theory provides some guidance on the dominant nucleation mode: whether impurity-mediated (heterogeneous) nucleation or homogeneous nucleation, by looking at the ratio of diffusion to adsorption rates. A large value of this ratio favors heterogeneous nucleation [50] because it ensures that fast migrating adatoms reach impurity sites very quickly, thus completing the nucleation process. This is especially true when the critical size is zero (as in the case impurity-mediated nucleation) where nucleation is deemed irreversible.

However, this same analysis could be problematic when applied to the system of study. Using the adsorption rate,  $F = 0.5$  ML/min and approximating the diffusion rate by considering only the dominant contribution from the easy diffusion direction: parallel to the Si dimer row where  $E_{||} = 0.31$  eV, we obtain a value of  $\sim 10^{11}$  for this ratio. Even though this is very high, one should not expect heterogeneous nucleation to dominate under all conditions owing to some peculiar attributes of the group III metal/Si(100) system. First, if nucleation on a C-defect is any guide, nucleation on impurity sites need not be irreversible. Second, as has been pointed out in [42] in the case of Ga on Si(100), aggregation is highly restricted to the reactive sites on either end of the islands (that is not already bound to a defect or impurity). This results in an elevated adatom density  $\sim 10^{-3}$  (per site) and persistent homogeneous nucleation even at adatom coverages above 0.1 ML (a regime where one might expect the island density to saturate before coalescence sets in).

We therefore propose that two characteristic features are key to the non-total dominance of heterogeneous nucleation. On the one hand, the fact that concentration of impurity is roughly two orders of magnitude higher at 0.15 H (per site) than the adatom density should favor heterogeneous nucleation. On the other hand, the degree of reversibility of H-mediated nucleation is largely governed by  $E_t$ . As we have seen in the simulations, this quantity is at most 0.2 eV (and most likely  $\sim 0.1$  eV); larger  $E_t$ 's result in greater composition of dimers among the islands and a feature not supported by experiment [22]. In fact, available experimental data seem to favor low  $E_t$ , which in turn should help suppress heterogeneous nucleation.

In Fig. 6a, we show simulated Al thin film morphology for  $E_t = 0.1$  eV. As discussed above, this value of  $E_t$  results in best agreement between simulation and experiment reported in Ref. [22] (optimum choice). Closer inspection of Fig. 6a reveal features that are consistent with experimental observations, such as the islands tending to have sizes  $< 5$  of which around 75% are dimers. (As mentioned previously

in the experiment detailed in Ref. [22], it was found that in some region of the H-dosed substrate, up to 75% of the islands are dimers). In the figure, we see that the majority of islands are heterogeneously nucleated (red-filled circles). This is in sharp contrast with Fig. 6b in which deposition of Al on clean Si(100) under identical growth conditions reveals islands (with density of around  $9.4 \times 10^{-3}$  per site) that are fewer (by a factor of 4) and longer. Additionally, we also simulated a model for which  $E_t = 0$  in order to determine the impact of suppressing impurity-mediated nucleation on the island density and the characteristics of the islands formed. The corresponding surface morphology is shown in Fig. 6c. While it also shows far more islands than that in the clean growth case shown in Fig. 6b by a factor of over 3 to 1, compared to Fig. 6a, it shows marginally larger islands which are homogeneously nucleated islands (black-filled circles). Consequently, dimers are also relatively fewer and comprise 62% of the islands on the surface.

#### 4. Conclusions

In summary, we have developed an atomistic lattice-gas model to simulate RT deposition of Al atoms in H-dosed Si(100) surface at submonolayer coverage using kinetic Monte Carlo techniques. Our DFT calculations reveal that the position of H relative to the Si dimer atoms ultimately dictates the preferential direction for heterogeneous island growth. Consequently these islands grow only on one side of H while growth on the other side is suppressed, a feature reminiscent of the growth of group III metals around C-defects on Si(100). Additionally, using DFT we determined the stabilities of end atoms in various H-bound Al island structures by calculating their adsorption energies. These calculations confirm that, in the presence of H atom, the Al adatom's gain in stability is minimal, though this structure becomes more stable with the addition of another adatom to form a (H-bound) metal dimer.

Using these results as a rough guide to the kMC simulations, along with prior experimental and theoretical observations from various studies, we found an almost fourfold increase in the island density on H-dosed Si(100) surface. We showed that part of this increase can be observed even when the largely immobile H-adatoms function in a mostly site-blocking role (i.e.  $E_t$  is close to 0). However, our analysis indicates that even a modest value of  $E_t$ , around 0.1 eV, improves agreement between model prediction and experiment on key quantities such as island density and percentage of islands that are dimers. Furthermore, our simulations predict that the density of homogeneous and heterogeneous islands should be comparable. In contrast, mean-field nucleation theory predicts that heterogeneous islands should dominate owing to the large ratio of diffusion to adsorption rate. The results of this study have wider implications on other

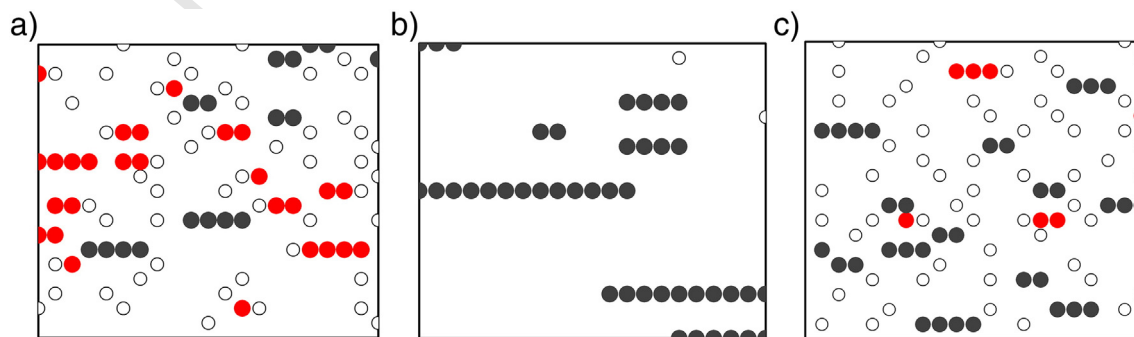


**Fig. 6.** (a) Al film formed at 373 K on Si(100)- $2 \times 1$  predosed with 0.15 ML of H showing predominantly H-bound islands (red solid circles) nucleating around H atoms (unfilled circles). These islands are shown to coexist with homogeneous islands (black solid circles). Here,  $E_t$  is set to the value that results in best agreement between model predictions and experimental data, i.e.  $E_t = 0.1$  eV. (b) In contrast, islands on clean Si(100)- $2 \times 1$  are much longer and almost exclusively homogeneously nucleated. A solitary C-defect (unfilled circle) is also shown. (c) Al film formed under identical growth conditions as in Fig. 6a, but with  $E_t = 0$ . Majority of islands shown here are homogeneous islands. Size of each simulated image above is  $7.68 \times 7.68$  nm<sup>2</sup>. (For interpretation of the references to color in this figure legend, the reader is referred to the web version of this article.)

metal-on-Si systems similarly dosed with “impurities”, a broad category to which residual H atoms and other types of surface defects belong. It suggests that while the mere presence of these impurities can increase the mean island density, such an increase may not always be directly attributed to impurity-mediated (heterogeneous) nucleation.

## 5. Uncited reference

[51]

## Acknowledgments

FCC and CHH were supported by the NCTS and the National Science Council of Taiwan under grant nos. NSC101-2112-M-110-002-MY3 and NSC101-2218-E-110-003-MY3. They are grateful to the National Center for High-performance Computing in Taiwan for the computer time and facilities.

## References

- [1] E. Dubois, J.-L. Bubbendorff, *Solid State Electron.* 43 (1999) 1085.
- [2] D. Wouters, U.S. Schubert, *Angew. Chem. Int. Ed.* 43 (2004) 2480.
- [3] A. Kühnle, *Curr. Opin. Colloid. Interface Sci.* 14 (2009) 157.
- [4] J. Schoiswohl, F. Mittendorfer, S. Surnev, M.G. Ramsey, J.N. Andersen, *F.P. Netzer, Surf. Sci.* 600 (2006) L274.
- [5] J. Nogami, A. Baski, C.F. Quate, *Phys. Rev. B* 44 (1991) 1415.
- [6] J. Nogami, A. Baski, C.F. Quate, *Phys. Rev. B* 43 (1991) 9316.
- [7] A. Baski, C.F. Quate, J. Nogami, *Phys. Rev. B* 44 (1991) 11167.
- [8] L. Jure, L. Magaud, J.M. Gomez-Rodriguez, P. Mallet, J.Y. Veuillen, *Phys. Rev. B* 61 (2000) 16902.
- [9] K.R. Simov, C.A. Nolph, Petra Reinke, *J. Phys. Chem. C* 116 (2012) 1670.
- [10] L. Jurczyszyn, M.W. Radny, P.V. Smith, *Surf. Sci.* 605 (2011) 1881.
- [11] C.A. Nolph, H. Liu, P. Reinke, *Surf. Sci.* 605 (2011) L29.
- [12] D.B. Putungan, H.J. Ramos, F.-C. Chuang, M.A. Albao, *Int. J. Mod. Phys. B* 5 (14) (2011) 1889.
- [13] A. Puchalska, A. Rakis, L. Jurczyszyn, M.W. Radny, *Surf. Sci.* 608 (2013) 188.
- [14] Y. Cui, J. Nogami, *Surf. Sci.* 605 (2011) 2038.
- [15] C. Eames, M.I.J. Probert, S.P. Tear, *Appl. Phys. Lett.* 96 (2010) 241903.
- [16] M. Dahne, Martina Wanke, *J. Phys. Condens. Matter* 25 (2013) 014012.
- [17] F. Leroy, J. Eymery, P. Gentile, F. Fournel, *Surf. Sci.* 545 (2003) 211.
- [18] J.W. Lyding, T.-C. Shen, J.S. Hubacek, J.R. Tucker, G.C. Abeln, *Appl. Phys. Lett.* 64 (1994) 2010.
- [19] J.W. Lyding, G.C. Abein, T.-C. Shen, C. Wang, J.R. Tucker, *J. Vac. Sci. Technol. B* 12 (1994) 3735.
- [20] J.W. Han, J.R. Kitchin, D.S. Sholl, *J. Chem. Phys.* 130 (2009) 124710.
- [21] B. Degroote, J. Dekoster, G. Langouche, *Surf. Sci.* 452 (2000) 172.

- [22] D.P. Adams, T.M. Mayer, B.S. Swartzentruber, *J. Appl. Phys.* 83 (1998) 4690. 602
- [23] S. Okano, S. Oshiyama, *Surf. Sci.* (2004) 272. 603
- [24] P. Kocan, P. Sobotik, I. Ostadal, J. Javorsky, M. Setvin, *Surf. Sci.* 601 (2007) 4506. 604
- [25] M.A. Albao, C.-H. Hsu, D.B. Putungan, F.-C. Chuang, *Surf. Sci.* 604 (2010) 396. 605
- [26] J.P. Perdew, K. Burke, M. Ernzerhof, *Phys. Rev. Lett.* 77 (1996) 3865. 606
- [27] P. Hohenberg, W. Kohn, *Phys. Rev. B* 136 (864) (1964); 607  
W. Kohn, L.J. Sham, *Phys. Rev.* 140 (1965) A1135. 608
- [28] G. Kresse, D. Joubert, *Phys. Rev. B* 59 (1999) 1758. 609
- [29] G. Kresse, J. Hafner, *Phys. Rev. B* 47 (558) (1993); 610  
G. Kresse, J. Furthmuller, *Phys. Rev. B* 54 (11 169) (1996) 11169. 611
- [30] T.C.G. Reusch, O. Warschkow, M.W. Radny, P.V. Smith, N.A. Marks, N.J. Curson, 612  
D.R. McKenzie, M.Y. Simmons, *Surf. Sci.* 601 (2007) 4036. 613
- [31] M. Mantega, I. Rugger, B. Naydenov, J.J. Boland, S. Sanvito, *Phys. Rev. B* 86 (2012) 614  
035318. 615
- [32] M.A. Albao, J.W. Evans, F.-C. Chuang, *J. Phys. Condens. Matter* 21 (2009) 405002. 616
- [33] P. Kocan, L. Jurczyszyn, P. Sobotik, I. Ostadal, *Phys. Rev. B* 77 (2008) 113301. 617
- [34] H. Itoh, J. Itoh, A. Schmid, T. Ichinokawa, *Phys. Rev. B* 48 (1993) 14663. 618
- [35] C. Zhu, S. Misawa, S. Tsukahara, *J. App. Phys* 80 (1996) 4205. 619
- [36] N. Takeuchi, *Phys. Rev. B* 63 (2000) 035311. 620
- [37] C. Polop, H. Hansen, W. Langenkamp, Z. Zhong, C. Busse, U. Linke, M. Kotrla, P.J. 621  
Feibelman, T. Michely, *Surf. Sci.* 575 (2005) 89. 622
- [38] This is a metastable state, and a third Al adatom placed at the M-site will remain 623  
there even upon relaxation using the quasi-Newton algorithm. 624
- [39] To preserve the anisotropic character of Si(100)-2 × 1, we introduce different 625  
values for the diffusion barrier along the two directions parallel and orthogonal 626  
to the Si dimer rows. 627
- [40] G. Brocks, P.J. Kelly, R. Car, *Phys. Rev. Lett.* 70 (1993) 2786. 628
- [41] D.D. Zorn, M.A. Albao, J.W. Evans, M.S. Gordon, *J. Phys. Chem. C* 113 (17) (2009) 629  
7277. 630
- [42] M.A. Albao, M.M.R. Evans, J. Nogami, D. Zorn, M.S. Gordon, J.W. Evans, *Phys. Rev. B* 631  
72 (2005) 035426. 632
- [43] T.-C. Shen, C. Wang, J.R. Tucker, *Phys. Rev. Lett.* 78 (1997) 1271. 633
- [44] C.J. Wu, I.V. Inova, E.A. Carter, *Phys. Rev. B* 49 (1994) 13488. 634
- [45] M.A. Albao, M.M.R. Evans, J. Nogami, D. Zorn, M.S. Gordon, J.W. Evans, *Phys. Rev. B* 635  
74 (2006) 0357402. 636
- [46] C.X. Zhu, S. Misawa, S. Tsukahara, A. Kawazu, S.J. Pang, *Appl. Phys. A Mater. Sci.* 637  
Process. 68 (1999) 145. 638
- [47] Assigning the same binding energy to an H-bound dimer as that used in other 639  
even-sized islands is one of the compromises in the model. A quick glance at 640  
Table 1, where it can be seen that the adsorption energy for H-bound dimer is 641  
greater by at least ~0.17 eV than the n = 4 case, makes it clear that its corre- 642  
sponding detachment rate is faster than that of the typical even-sized island. 643  
However, the impact of the reduced binding energy (if implemented in the 644  
model) would be a slight decrease in the number of heterogeneous islands. 645
- [48] To mimic actual experimental condition, we assume a small amount of C-defects 646  
(~0.003 per site) are present on the clean Si(100) surface, and just like H atoms 647  
they can similarly trap Al adatoms, albeit more weakly. Under these assumptions 648  
and taking into account the results in [51], we estimate that the Al island density 649  
at 373 K is  $9.4 \times 10^{-3}$  per site. 650
- [49] J. Javorsky, M. Setvin, I. Ostadal, P. Sobotik, M. Kotrla, *Phys. Rev. B* 79 (2009) 651  
165424. 652
- [50] R. Vardavas, C. Ratsch, R.E. Catflisch, *Surf. Sci.* 569 (2004) 185. 653
- [51] C. Zhu, S. Misawa, S. Tsukahara, S. Fujiwara, *Surf. Sci.* 357–358 (1996) 926. 654